Indications of Nuclear-Track-Guided Electrons Induced by Fast Heavy Ions in Insulators

G. Xiao,[1] G. Schiwietz,[1] P. L. Grande,[2] N. Stolterfoht,[1] A. Schmoldt,[1]
M. Grether,[1] R. Köhrbrück,[1] A. Spieler,[1] and U. Stettner[1]

[1]*Hahn-Meitner-Institut, Bereich Festkörperphysik, Glienicker Str. 100, 14109 Berlin, Germany*
[2]*Instituto de Física, Universidade Federal do Rio Grande do Sul, 91500 Porto Alegre, Brazil*

We present experimental evidence for a deceleration of convoy electrons produced by 5 MeV/u ions (N^{7+}, Ne^{10+}, S^{13+}, Ni^{23+}, and Ag^{37+}) during the interaction with insulator foils at normal incidence. The deceleration first increases with increasing projectile charge, reaches a maximum at a projectile charge of about 16, and seems to approach zero for even higher charges. Different possible mechanisms and quantitative estimates for the slowing down of convoy electrons are presented. [S0031-9007(97)03999-9]

Electron spectra in ion-solid interactions show, apart from Auger lines and binary-encounter electrons, one prominent structure exactly in the projectile flight direction: the convoy-electron peak. Convoy electrons are fast electrons that leave the solid surface with about the same velocity as the projectile ion. They give rise to a cusp shaped kinematic peak and are related to the attractive Coulomb potential of positive ions. This peak was first measured in ion/atom collisions experiments [1] and shortly after for ion-solid interactions [2]. In both cases convoy electrons are produced by electron capture (ECC) [3] and by electron loss to continuum states of the projectile (ELC) [4,5]. In dense matter, these electrons are subject to a random walk under the influence of the target constituents and the projectile potential [6].

Convoy electrons can be accelerated by the image-potential of the projectile charge, as has been found for ions under glancing-angle scattering conditions at semiconductor and metal targets [7–9] and at normal-incidence conditions for highly charged ions at a proton-equivalent energy of 5 MeV/u [10]. In ion-insulator interactions ionizing collisions result in a positive nuclear-track potential, which can decelerate target Auger-electrons emitted from the insulator surface [11] and accelerate desorbed positive hydrogen ions [12]. In this Letter we present first evidence for a *deceleration of convoy electrons* induced by 5 MeV/u highly charged ions traversing insulating polypropylene ($[C_3H_6]_n$) foils at normal incidence.

A detailed description of the experimental setup has been published previously [10,11]. 5 MeV/u heavy ions were delivered by the heavy-ion cyclotron of the Ionenstrahl-Labor (ISL) at the Hahn-Meitner Institut. The beam was sent through a post-cyclotron stripper foil and a magnet to select projectiles with a charge-state close to equilibrium. The beam of 0.1 to 10 particle nA was collimated to about 1 mm² at the center of the magnetically shielded target chamber with a vacuum of typically 10^{-6} mbar. During the experiments the targets were wobbled in both directions perpendicular to the beam for an accurate fluence determination and

for a reduction of the heat load. For the measurement of convoy-electron spectra an electrostatic zero-degree tandem spectrometer (energy resolution $\Delta E/E = 0.6\%$ and solid angle $\Delta\Omega = 2 \times 10^{-5}$ sr) was used [13]. The ions pass the first stage of the spectrometer and electrons emitted in the beam direction are deflected into a second stage, where they are analyzed according to their energy. Samples of polypropylene (PP) foils were stretched to a thickness of 1.5 μm and prepared by deposition of an Al coating of 20 μg/cm² on one side of the foil, so that a maximum temperature rise of less than 50 K for the highest ion flux during the irradiation is expected inside the PP substrate. With this coating there was nearly no macroscopic charging for heavy ions. Width and position of the target-Auger peak, convoy peak, and total electron yields for different ion currents are consistent with <3 V for fluctuations and <20 V for the absolute macroscopic charging [10,11].

Figure 1 shows the convoy-electron spectra for 5 MeV/u Ni^{23+} ions penetrating PP foils at two orientations: with the evaporated Al layer in beam direction and opposite to the beam direction [Figs. 1(a) and 1(b)]. The structures on the wings of the peak are due to autoionization of the low energetic projectile states $1s^2 2s2pnl$ and $1s^2 2pnl$. The thick solid curves in Figs. 1(a) and 1(b) are the spectra for 8 μg/cm² Al and 100 μg/cm² carbon foils, respectively. The data points and smoothed thin solid curves represent the convoy-electron spectra for the PP/Al-film targets. It is seen that these spectra shift to higher energies with increasing ion fluence. There are a few effects that influence the convoy-electron energy. First, highly charged ions produce multiple bond breaking along the track. Correspondingly, a large number of hydrocarbon molecules, and also hydrogen, are released through the PP surface; the so-called carbonization process. Hence, the foil thickness and the projectile energy loss are reduced, resulting in an increase of the convoy-electron energy for both foil orientations. Secondly, convoy electrons near to the PP surface are influenced by a possible positive macroscopic charging-up
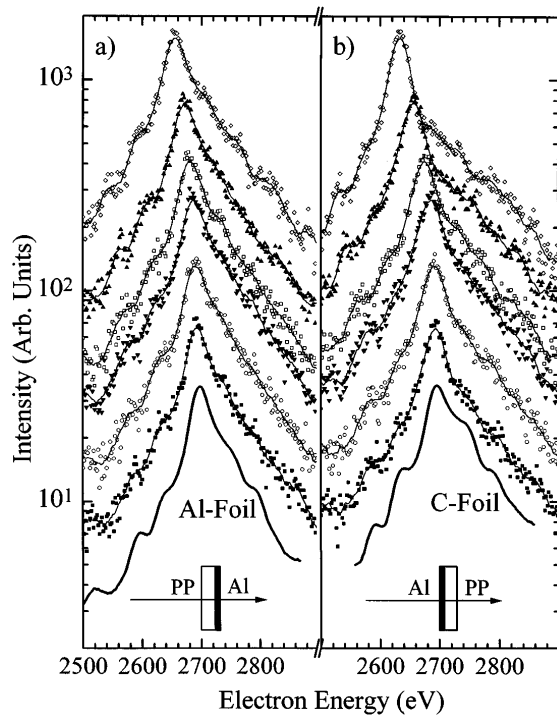
FIG. 1. Convoy-electron spectra for 5 MeV/u Ni^{23+} + PP/Al foils (1.5 μm PP + 20 μg/cm^2 Al), multiplied by arbitrary factors. The plot symbols and thin solid lines (smoothed spectra) correspond to fluences from 2×10^{12} (upper spectra) to 3×10^{13} ions/cm^2 (lower spectra). The spectra at the bottom (thick solid lines) are taken for an Al foil and an amorphous carbon foil, respectively.

V_{mac}. Finally, the projectile ions induce a negative image potential on the Al surface and a positive nuclear-track potential inside the bulk as well as on the surface of PP.

For thin carbon and Al foils autoionization takes place far beyond the exit surface of the foil. The emission of slow autoionizing electrons in the projectile system results in two distinct lines in the laboratory frame, corresponding to forward and backward emission. From these two lines the projectile velocity can accurately be determined [10,13]. This method will be denoted *Auger method* and it directly yields the energy shift of convoy electrons. Another method of determining the convoy-energy shift is the *solid/gas method*. Here, the convoy peak position is measured for a thin gas target (the peak coincides with the projectile velocity) as well as for foils of different thickness. Extrapolation to zero foil thickness enables one to determine the influence of solid-state effects on the convoy-electron energy [10].

The absolute microscopic convoy-energy shift for polypropylene ΔE(PP) may be deduced from the microscopic shift for the conducting Al surface ΔE(Al) as

$$\Delta E(\text{PP}) = \Delta E(\text{Al}) + \Delta E_{\text{diff}} + V_{\text{mac}}e, \qquad (1)$$

where ΔE_{diff} is the energy difference for the PP and the Al surface of the samples, extrapolated to zero fluence. This method of determining absolute microscopic

energy shifts for thick foils will be named the *surface/surface* method, since it is based on a comparison of the two surfaces (Al and PP) of a sample. Using the *Auger method* it was found ΔE(C) $\approx \Delta E$(Al) to within 0.5 eV for Ni^{23+} ions. Thus, we replace ΔE(Al) in Eq. (1) by the interpolated values of ΔE(C) for all ions. For the determination of V_{mac} we have used the PP electron spectra below 40 eV. Initially, these spectra show a significant reduction of the yield compared to high fluences (without macroscopic charging) or the carbon data. Accounting for an energy shift and refraction at a macroscopic planar potential the high-fluence spectra at low energies could be well fitted to the low-fluence spectra using only V_{mac} as free parameter. For PP we derived $V_{\text{mac}} = 9 \pm 3$ V extrapolated to zero fluence, without a significant dependence on the projectile charge or on the beam current [10].

Figure 2 displays the convoy energy shifts as a function of the projectile atomic number Z_p. Using the solid/gas method and the Auger method the carbon data have already been evaluated and published previously
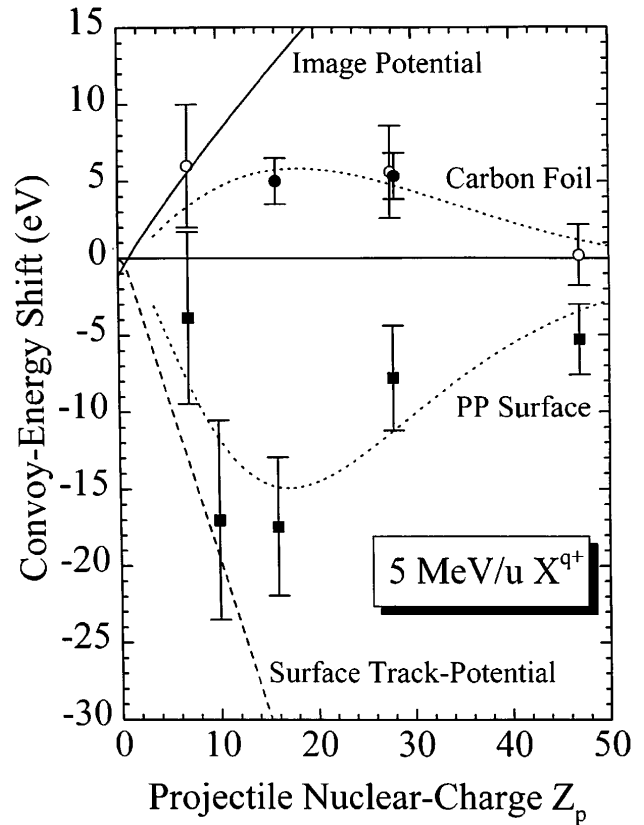

FIG. 2. Energy shifts of convoy electrons for 5 MeV/u ions with respect to the projectile speed versus the projectile atomic number. The open circles, the closed circles, and the closed squares are obtained with the solid/gas method, the Auger method, and the surface/surface method, respectively (dotted curves to guide the eye). The solid line represents the dynamic image potential using the model of Refs. [14,15] and the dashed line shows an estimate for the maximum surface track-potential after the ion has left the insulator [11].

[10]. For Ni^{23+} ions both methods were used and the results are consistent with each other. It is seen that there is an *acceleration* of convoy electrons for the amorphous carbon target. Contrary to the carbon results, the measured microscopic energy shift for PP (closed squares), corresponds to a *deceleration* of convoy electrons. These data were determined with the surface/surface method in the limit of low fluences. The dashed line represents an estimate of the surface track potential (half the theoretical bulk value [11]), resulting from positively charged target atoms along the track.

The deceleration for PP as well as the acceleration for C foils appear to vanish in the limit of high Z_p. This common feature might be related to an increasing Coulomb attraction that suppresses any influence of solid-state potentials on the convoy-electron energy. For high Z_p it is possible that solid-state potentials saturate and/or that the convoy electron cloud is compressed near the nucleus leading to an over-proportional projectile attraction. Previous investigations indicate that the acceleration observed for the conducting target is due to the influence of the image potential of the projectile/convoy-electron system [7,8]. In fact, for low projectile charges the calculated image potential (solid line [14,15]) is consistent with the shifts measured for C foils. Figure 2 suggests that the deceleration observed for PP is linked in a similar way with the surface contribution of the nuclear-track potential. As will be discussed in the following, however, this is not the case and a new mechanism has to be considered.

Burgdörfer *et al.* have shown that the main features of convoy-electron ejection can be incorporated in a classical transport model [6]. However, these classical-trajectory Monte Carlo (CTMC) calculations are very time consuming and, hence, cannot be applied to our collision systems with low convoy-electron yields. Previously we have performed semianalytical calculations for the penetration of a projectile-centered charge cloud through a surface step-potential [10]. In the present work, we have extended these calculations by allowing for a simultaneous interaction of convoy electrons with the projectile Coulomb field as well as with a planar surface potential of finite range. For this purpose a CTMC code for the electronic motion in the combined field of two spherical potentials [16] was modified.

With realistic values for the surface potential, for its range and for the radial extension of the convoy-electron distribution, we have computed unique cusp shapes similar to the ones in Fig. 1. Only for unrealistic strong potentials exceeding a few hundred V or for radial extensions exceeding 50 a.u. at the surface, we found significant changes of the peak structure and also a shift of the convoy peak position. From the above discussion it follows that the short-ranged (10 Å) nuclear-track potential at the surface has no significant influence on the convoy-electron energy and possible long-range contributions due to vacancies from fast emitted electrons

are less than 5 eV at $Z_p < 20$. Thus, the observed deceleration appears to be no surface effect.

Hence, we infer that the deceleration is a bulk effect that is present in PP but not in conducting materials. In fact, the slow electron recombination in PP gives rise to a strong positive nuclear-track potential that can influence the convoy-electron emission. At a distance of about 50 Å behind the projectile a long lived cylindrical potential evolves as a result of target ionization along the projectile path [10,11]. In contrast to the model of wake-riding electrons in metals [17], the nuclear-track potentials may induce a channeling-like motion of quasi-free electrons that move behind the projectile. Such *nuclear-track guided electrons* will predominantly be emitted at 0° somewhat below the convoy-electron velocity, since projectile-centered electrons may easily be caught in the dynamic track potential behind the projectile and slow down by interactions with other electrons of the medium. The track-guided electrons should give rise not only to a reduction of the apparent convoy-electron energy, but also to an enhancement of the convoy-electron yield.

Figure 3 shows the ratio of the convoy-electron yields for PP and C as function of Z_p and for low as well as for high fluences of $(2-5) \times 10^{16}/Z_p^2$ (ions/cm²), where the relative hydrogen content is reduced by about 20% (carbonization). Under this condition the conductivity is increased by some orders of magnitude and electron recombination is much faster than for untreated PP samples. Correspondingly, the target-Auger spectra as well as the convoy electron spectrum for PP at this fluence can barely be distinguished from the carbon data. Thus,
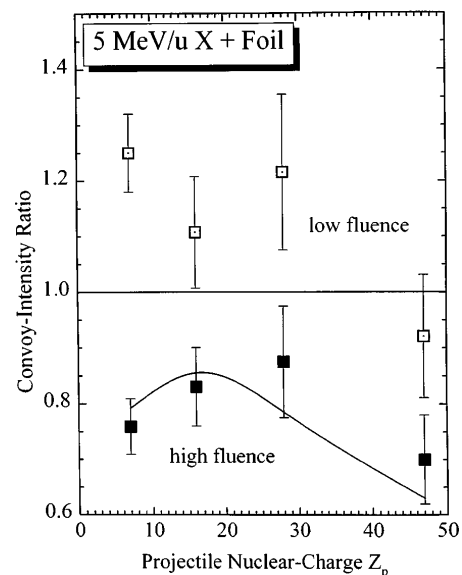

FIG. 3. Ratio of convoy-electron intensities for polypropylene (PP) and amorphous carbon targets versus the projectile nuclear-charge. The PP data have been determined for different fluences and the C-foil data show no fluence dependence. The theoretical prediction (solid line) is explained in the text.

the high-fluence data are representative for a hydrocarbon compound similar to PP, but without any influence of the nuclear-track potential.

The solid line in Fig. 3 represents model calculations for the relative convoy-electron yield using the rate-equations program by Rozet *et al.* [18]. This code uses basic ion-atom collision cross sections to calculate the mean charge state of heavy ions in solids and the results are in good agreement with our experimental data for 5 MeV/u ions. Here we simply use the calculated population of the $n = 3$ level to estimate the Rydberg-state population per energy interval and the corresponding convoy-electron density. The calculated ratio of PP and carbon foil results should be highly accurate, since the electron-capture processes are dominated by the contribution from the carbon K shell and the projectile-ionization cross sections are modified by less than 25% due to the presence of hydrogen atoms in PP. As can be seen from Fig. 3, there is good agreement between the model results and the high-fluence PP data which correspond to a hydrocarbon compound with enhanced recombination speed. The low-fluence PP data have been extrapolated to zero fluence and the main difference to the high-fluence data in Fig. 3 should be the slow electron recombination in the untreated PP sample (before irradiation). Comparison with the high-fluence data or with the theoretical prediction shows a 30% to 50% increase of the convoy-electron yield. This points to an additional mechanism for the production of convoy electrons in insulators and it is proposed that this mechanism is the ejection of the above discussed track-guided electrons.

In conclusion, convoy-electron emission has been investigated experimentally and theoretically for heavy-ion irradiation of conducting and insulating solid-state targets at a particle velocity of 14.1 a.u. For the insulating polypropylene target we found a reduced energy of convoy electrons as well as an increased electron yield in comparison to a conducting target. Model calculations show that the measured deceleration cannot be explained as a surface effect. It is thus proposed that, additionally to the "standard" convoy electrons, there is a considerable fraction of nuclear-track guided electrons emitted close to the convoy-electron velocity. The high ionization density in the solid leads to an attractive potential that may guide electrons preferentially in the zero-degree direction. Since these track-guided electrons are initially created during the transport of convoy electrons deep inside the solid, they suffer additional energy losses as they move far behind the projectile, and thus they appear at velocities somewhat below the projectile velocity. The measured electron yield as well as the energy shift appear to be reasonable for the proposed process, but it would be desirable to compare with more refined model calculations.

We are indebted to J. P. Rozet for his rate-equations code and to A. Arnau and J. Burgdörfer for fruitful

---

[1] G. B. Crooks and M. E. Rudd, Phys. Rev. Lett. **25**, 1599 (1970).

[2] K. G. Harrison and M. W. Lucas, Phys. Lett. **33A**, 142 (1970).

[3] A. Salin, J. Phys. B **2**, 631 (1969).

[4] D. Burch, H. Wieman, and W. B. Ingalls, Phys. Rev. Lett. **30**, 823 (1973).

[5] M. Breinig, S. B. Elston, S. Huldt, L. Liljeby, C. R. Vane, S. D. Berry, G. A. Glass, M. Schauer, I. A. Sellin, G. D. Alton, S. Datz, S. Overbury, R. Laubert, and M. Suter, Phys. Rev. A **25**, 3015 (1982).

[6] J. Burgdörfer, *Lecture Notes in Physics,* edited by D. Berenyi (Springer, Berlin, 1987), Vol. 294, pp. 344; J. Burgdörfer and C. Bottcher, Phys. Rev. Lett. **61**, 2917 (1988).

[7] K. Kimura, M. Tsuji, and M. Mannami, Phys. Rev. A **46**, 2618 (1992); K. Kimura, T. Kishi, and M. Mannami, Nucl. Instrum. Methods **B90**, 282 (1994).

[8] A. Koyama, Y. Sasa, H. Ishikawa, A. Misu, K. Ishii, T. Iitaka, Y. H. Ohtsuki, and M. Uda, Phys. Rev. Lett. **65**, 3156 (1990); H. Ishikawa, A. Misu, A. Koyama, T. Iitaka, M. Uda, and Y. H. Ohtsuki, Nucl. Instrum. Methods **B67**, 160 (1992).

[9] E. A. Sánchez, O. Grizzi, G. Nadal, G. Gómez, M. L. Martiarena, and V. H. Ponce, Nucl. Instrum. Methods **B90**, 261 (1994).

[10] G. Xiao, G. Schiwietz, P. L. Grande, A. Schmoldt, M. Grether, R. Köhrbrück, N. Stolterfoht, A. Spieler, and U. Stettner, Nucl. Instrum. Methods **B115**, 215 (1996); G. Schiwietz, G. Xiao, P. L. Grande, A. Schmolt, M. Grether, R. Köhrbrück, A. Spieler, and U. Stettner, Scanning Microsc. Int. (to be published).

[11] G. Schiwietz, P. L. Grande, B. Skogvall, J. P. Biersack, R. Köhrbrück, K. Sommer, A. Schmoldt, P. Goppelt, I. Kádár, S. Ricz, and U. Stettner, Phys. Rev. Lett. **B69**, 628 (1992); G. Schiwietz and G. Xiao, Nucl. Instrum. Methods **B107**, 113 (1996).

[12] K. Wien, Ch. Koch, and Nguyen van Tan, Nucl. Instrum. Methods **B100**, 322 (1995).

[13] A. Itoh, T. Schneider, G. Schiwietz, Z. Roller, H. Platten, G. Nolte, D. Schneider, and N. Stolterfoht, J. Phys. B **16**, 3965 (1983).

[14] P. M. Echenique and R. H. Ritchie, Phys. Rev. B **20**, 2567 (1979).

[15] J. Burgdörfer, Nucl. Instrum. Methods **B24/25**, 139 (1987).

[16] V. J. Montemayor and G. Schiwietz, J. Phys. B **22**, 2555 (1989).

[17] M. H. Day, Phys. Rev. Lett. **44**, 752 (1980).

[18] J. P. Rozet, A. Chetioui, P. Piquemal, D. Vernhet, K. Wohrer, C. Stéphan, and L. Tassan-Got, J. Phys. B **22**, 33 (1989).